Korean J. Chem. Eng., 38(6), 1197-1204 (2021)
DOI: 10.1007/s11814-021-0769-5

pISSN: 0256-1115
eISSN: 1975-7220

Selective hydrogen combustion over Rh-Sn/Al_2O_3 catalysts during propane dehydrogenation

Jae-Won Jung*, Kyeongseok Oh, Kwang-Deog Jung***,†, Won Il Kim****, and Hyoung Lim Koh*,†**

*Department of Chemical Engineering, RCCT, Hankyong National University, Anseong 17579, Korea
**Chemical and Environmental Technology Department, Inha Technical College, Inha-ro 100, Michuhol-gu, Incheon 22212
***Clean Energy Research Center, Korean Institute of Science and Technology,
P. O. Box 131, Cheongryang, Seoul 02792, Korea
****R&D Business Lab., Hyosung Co., 74 Simin-daero, Dongan-gu, Anyang, Gyeounggi 14080, Korea
(*Received 30 November 2020 • Revised 10 February 2021 • Accepted 23 February 2021*)

Abstract−A series of Rh-Sn/Al_2O_3 catalysts were prepared by 0.5 wt% of Rh and varied amounts of Sn from 0 to 3.0 wt%. Rh-Sn catalysts were evaluated to determine if selective hydrogen combustion(SHC) can be effectively applicable to propane dehydrogenation (PDH). PDH is an endothermic reaction and SHC can generate partial heat energy. In this study, two separate SHC reactions were examined. One was to look into the quantification of competitive combustion states over Rh-Sn catalysts in the presence of hydrogen, propylene, oxygen, and nitrogen. The other was to evaluate SHC with Rh-Sn catalysts in the presence of hydrogen, propane, oxygen, and nitrogen. The factor that we entitled A factor, was employed to analyze the effect of Sn amount. The result showed that the best performance was achieved by 0.5Rh-1.5Sn/Al_2O_3 catalyst for both SHC reactions. Characteristics of catalysts were analyzed by CO chemisorption, XPS, TEM-EDX and TPR.

Keywords: Rh-Sn/Al_2O_3, Selective Hydrogen Combustion, Hydrogen Conversion, Propane Dehydrogenation, Sn Effect

INTRODUCTION

In the petrochemical industry, olefins are basic compounds mainly produced by either naphtha steam cracking or catalytic cracking. As the demand for specific olefins increased, olefins individually from the dehydrogenation of ethane, propane and butane also became popular [1-4]. It is known that propylene production by propane dehydrogenation (PDH) is generally an endothermic reaction when a metal catalyst such as platinum is used. The reaction scheme of PDH is shown below.

$$C_3H_8 \leftrightarrow C_3H_6+H_2,\ \Delta H_{298}=+129\ kJ/mol \quad (1)$$

A higher conversion rate of propane requires high temperature and low pressure [5]. In addition, it was reported that the major side reactions during PDH reaction are undesirable cracking and/or hydrocracking of propane. Both reactions are presented below.

$$C_3H_8 \leftrightarrow CH_4+C_2H_4,\ \Delta H_{298}=+79.4\ kJ/mol \quad (2)$$

$$C_3H_8+H_2 \leftrightarrow C_2H_6+CH_4,\ \Delta H_{298}=-63.4\ kJ/mol \quad (3)$$

Among the commercial catalysts, Pt catalyst is most popular in PDH. When Pt catalyst is employed for PDH, Sn is used as a co-catalyst in order to inhibit the unwanted hydrogenation reaction [6]. Nevertheless, side reactions of hydrogenation still occur [7]. Unfortunately, it is still hard to sustain PDH for a long period of time because almost uncontrollable reactions occur, which includes the reactions of (1), (2), and (3) listed above. In the presence of hydrogen during PDH, hydrogenation and several reactions occur simultaneously even in the same active site of catalyst [8]. Various studies attempted to apply oxidation reaction to PDH using gas phase oxygen or lattice oxygen from oxides [8-13]. One of suggested concepts, selective hydrogen combustion (SHC), was introduced earlier [13]. In the SHC reaction, only hydrogen is selectively burned using oxygen. Hydrogen is the major product with propylene during PDH reaction. In addition, SHC accelerates the equilibrium conversion rate by inducing the equilibrium state of PDH reaction to the right hand side in reaction (1). SHC also increases the energy efficiency of overall PDH reaction by using the heat of combustion. Although SHC has not been commercialized to PDH process, the successful application of SHC into the dehydrogenation of ethylbenzene has been imported [13]. Since PDH is generally operated in a relatively high temperature up to 620 °C [5,14-16], SHC with sacrificing propane and propylene less would be required. Application of suitable catalysts will be the essential task for SHC. In previous researches, Pt, Au and Rh over supportive oxides such as In_2O_3 and Bi_2O_3 were used for SHC candidate catalysts [8,12,17-22]. Blekkan and coworkers [8,12] explored Pt and metal oxide catalysts, and Ping Li et al. [11,23] reported the effect of support. It was noticeable that Grasselli et al. suggested metal oxides and supports [18].

In this paper, two separate SHC reactions were performed to evaluate the catalytic activity at 550 °C. At first, SHC experiment was conducted in the presence of hydrogen, oxygen and propylene. Second, SHC was performed in the presence of hydrogen, propane, oxygen, which includes PDH as well. A series of Rh-Sn catalysts were prepared by 0.5 wt% of Rh and varied amount of Sn from

†To whom correspondence should be addressed.
E-mail: jkdcat@kist.re.kr, hlkoh@hknu.ac.kr

0.5 to 3.0 wt% over alumina support. Sn effect was also evaluated in both cases. Characteristics of catalysts were investigated by CO chemisorption, transmission electron microscopy (TEM) combined with energy dispersion spectroscopy (EDS), X-ray photoelectron spectroscopy (XPS), and temperature programmed reduction (TPR).

EXPERIMENTAL

1. Catalyst Preparation

Rhodium (III) chloride hydrate ($RhCl_3 \cdot 3H_2O$, Sigma Aldrich) and stannous chloride ($SnCl_2$, Sigma Aldrich) were used as metal precursors for the supported Rh-Sn catalysts. Al_2O_3 (γ-Al_2O_3, supplied by BASF) was used as a catalyst support. $RhCl_3 \cdot 3H_2O$ and $SnCl_2$ were dissolved in ethanol (C_2H_5OH, 99.5%, Daejung), and Al_2O_3 was co-impregnated with these precursors. The co-impregnated Rh-Sn/Al_2O_3 catalyst (Rh-Sn catalyst) was dried at 120 °C for 12 h and calcined at 600 °C for 3 h in air. The Rh content was fixed as 0.5 wt%, while the Sn content was varied as 0, 0.15, 0.3, 0.5, 0.75, 1.0, 1.5, 2.0 and 3.0 wt%, which are labeled to 0.5Rh, 0.5Rh-0.15Sn, 0.5Rh-0.3Sn, 0.5Rh-0.75Sn, 0.5Rh-1.0Sn, 0.5Rh-1.5Sn, 0.5Rh-2.0Sn, and 0.5Rh-3.0Sn, respectively. Monometallic 1.5Sn catalyst was also used.

2. Catalytic Activity Measurements

Two separate SHC reactions were performed at 550 °C. The catalytic activity during SHC reactions was evaluated in a fixed-bed reactor (quartz, inner diameter: 18 mm) using 0.1 g of each catalyst. Before each SHC reaction, a series of Rh-Sn catalysts were reduced at 550 °C in the presence of H_2 (30 mL/min) and N_2 (70 mL/min). Compositions and flow rates of gaseous feed are summarized in Table 1. The first SHC reaction (SHC-1) was carried out for 5 h under atmospheric pressure in the presence of C_3H_6 (10 mL/min), H_2 (10 mL/min), O_2 (5 mL/min) and N_2 (75 mL/min). And a second SHC reaction (SHC-2) also carried out at 550 °C for 2 h under atmospheric pressure in the presence of C_3H_8 (10 mL/min), H_2 (10 mL/min), O_2 (5 mL/min) and N_2 (75 mL/min). The difference between two SHC reactions is in the usage of different hydrocarbons, propylene versus propane. The reaction product was collected at various time intervals and analyzed by gas chromatography (TCD, 5890 Series2 Plus, Hewlett Packard, USA) using a 50 m×0.53 mm Carboxen 1010 capillary column. The determined values were reproducible within acceptable error ranges (less than 5%) based on authors' experience.

3. Characterization

TEM images were obtained using an FEI Tecnai G2-20 S-Twin operating at an accelerating voltage of 200 kV. TEM mapping images were obtained using an FEI transmission electron microscope. To analyze chemical states of the elements, X-ray photoelectron spectroscopy (XPS) was performed using an AXIS Nova spectrometer (Kratos, UK) equipped with a monochromatic electroanalyzer and a monochromatic Al-Kα 150 W X-ray source. Metal dispersion was measured by CO chemisorption using a Micromeritics ASAP2020C volumetric analyzer. A fixed amount of each catalyst (0.5 g) was treated under a He gas flow at 110 °C for 0.5 h. Subsequently, the pretreated catalysts were heated from room temperature to 350 °C under a pure H_2 flow for 3 h. In the subsequent reduction, a purge step was performed under a He gas flow at the same temperature for 2 h. Then, the sample was cooled to 35 °C and purged under a He gas flow for 2 h. After pretreatment, the catalyst was subjected to a flow of CO as an adsorbate for total adsorption measurements. Afterward, the catalyst was evacuated to remove the physically adsorbed CO, and CO flow was initiated again for physical adsorption measurements. The amount of chemisorbed CO was determined by analyzing the difference between the two quantities of the adsorbed CO. The reducing properties of the catalyst were investigated by a temperature program reduction (TPR) method. The experiment was carried out with an automatic chemical adsorption analyzer equipped with a TCD detector. The sample (0.1 g) was embedded in a U-shaped quartz tube between two containments of quartz wool. Before TPR measurement, each sample was pretreated with a flow of high purity Ar at 30 ml/min for 2 hours at 150 °C. The sample was then cooled to 40 °C and flushed continuously with a 30 ml/min Ar flow. Thereafter, TPR measurement was performed at a flow rate of 30 ml/min of 10% H_2/Ar, and the temperature of the sample was increased from 40 °C to 800 °C at a rate of 10 °C/min.

Table 1. Compositions and flow rates of gaseous feed

Composition of gaseous feed for SHC-1	Composition of gaseous feed for SHC-2	Flow rate (mL/min)
C_3H_6	C_3H_8	10
H_2	H_2	10
O_2	O_2	5
N_2	N_2	75

RESULTS AND DISCUSSION

1. Catalytic Performance for SHC-1 Reaction in Propylene

For SHC-1 reaction, a series of Rh-Sn catalysts including 0.5Rh and 1.5Sn were used, respectively, at 550 °C. Feed flows were controlled as presented earlier in Table 1. Propylene, hydrogen, oxygen, and nitrogen were used. Note that the volumetric flow rate of oxygen was set to a half of hydrogen inlet. Fig. 1 shows the propyl-

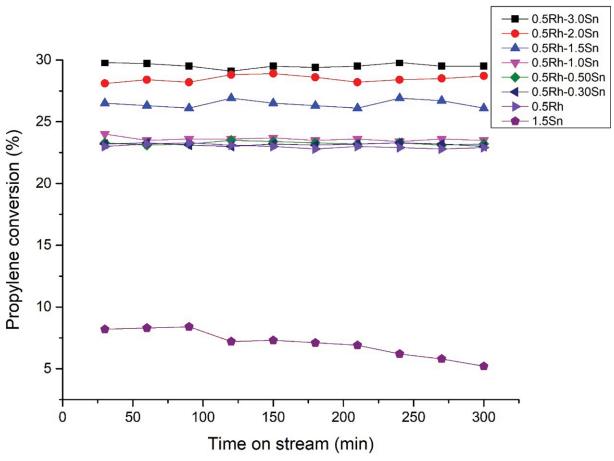

Fig. 1. Propylene conversion over a series of Rh-Sn catalysts.

Table 2. Reaction results over H_2 conversion, O_2 conversion, and propylene conversion (SHC-1)

Catalysts	H_2 conversion (%)	O_2 conversion (%)	Propylene conversion (%)
0.5Rh	62.0	91.0	23.0
0.5Rh-0.3Sn	63.7	95.0	23.2
0.5Rh-0.5Sn	63.6	94.9	23.3
0.5Rh-1.0Sn	65.2	94.8	24.0
0.5Rh-1.5Sn	77.7	94.8	26.5
0.5Rh-2.0Sn	78.0	95.0	28.1
0.5Rh-3.0Sn	80.0	96.0	29.8
1.5Sn	20.6	95.0	8.2

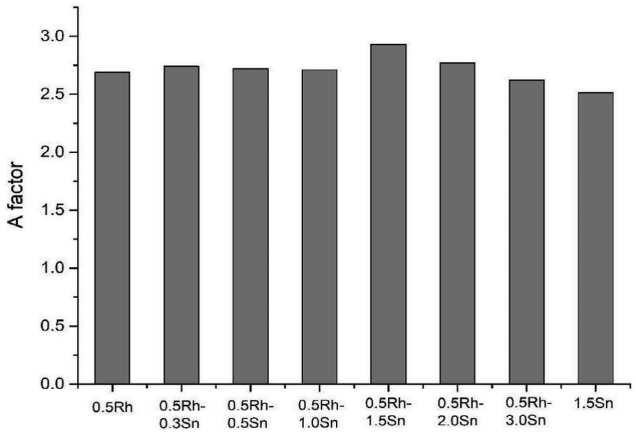

Fig. 2. Calculated A factor from Rn-Sn catalysts in the presence of propylene, hydrogen, oxygen and nitrogen (SHC-1).

ene conversions from Rh-Sn catalysts during SHC-1 reaction. The best activity was achieved with 0.5Rh-3.0Sn catalyst, while the least activity was observed in 1.5Sn catalyst. It was noticeable that there is no deteriorated trend in propylene conversion data for 300 min. The order by propylene conversion data was as follows: 0.5Rh-3.0Sn>0.5Rh-2.0Sn>0.5Rh-1.5Sn>0.5Rh-1.0Sn>0.5Rh-0.5Sn≃0.5Rh-0.3Sn≃0.5Rh>>1.5Sn. It was clear that more Sn addition over Rh catalyst showed the better performance in propylene conversion during SHC-1 reaction.

In Table 2, presented are the conversion data of H_2, O_2, and propylene for SHC-1 reaction. The range of H_2 conversion was recorded from 62 to 80% in Rh-Sn catalysts, and the increase of H_2 conversion with increasing Sn amounts was observed. In particular, the sharp increase of H_2 conversion started from 0.5Rh-1.5Sn catalyst after mild increase in lower Sn addition. However, no further sharp increase was observed in H_2 conversion data for 0.5Rh-2.0Sn and 0.5Rh-3.0Sn. Supplementary, H_2 conversion was 20.6% with monometallic 1.5Sn catalyst. It supports the fact that hydrogen may adsorb on the surface of Sn oxides, either SnO or SnO_2. In terms of O_2 conversion, all catalysts showed higher values from 91 to 96%. It implies that the adsorption of O_2 may occur equally on all metal species regardless of active Rh or less active Sn oxides [24]. The phases of Sn were determined to SnO as well as SnO_2, which will be discussed later in the XPS section. It was suspected that there was no significant difference between the degree of adsorption of O_2 over the surfaces of either SnO or SnO_2 in this work. The increasing trend of propylene conversions was also noticed with increasing Sn amount. Even 1.5Sn catalyst showed 8.2% of propylene conversion, which may have been induced by oxygen moieties adsorbed on the surface of 1.5Sn catalyst.

In Table 3, generated products were analyzed with respect to carbon balance. Initial carbon source is propylene only. During SHC-1 reaction, carbons in propylene converted to CO, CO_2, methane, ethane, ethylene, and propane. The combined amount of CO and CO_2 was approximately in the range of 53.5-57.1% from 0.5Rh to 0.5Rh-1.0Sn catalysts. Interestingly, the generation of CO and CO_2 was suddenly decreased at 0.5Rh-1.5Sn catalyst. Recall Table 2, 0.5Rh-1.5Sn showed the increase of propylene conversion, which should be carefully analyzed. It shows that the total consumption of propylene contributes two ways: combustion and hydrogenation. Here, hydrogenation includes the generation of methane, ethane, ethylene, and propane. The objective of this study was to achieve the optimized selective hydrogen combustion. If PDH occurs, hydrogen combustion may lead the return of propane from converted propylene. Nevertheless, it will be attributed to reducing the total combustion of carbons. The highest value in propane generation in 0.5Rh-1.5Sn may be interpreted by effective metal dispersion, which will be discussed later in CO chemisorption section.

In Fig. 2, we labeled the A factor for the ratio of H_2 conversion to propylene conversion and presented with respect to Rh-Sn catalysts. The term, A factor, was introduced in an earlier research paper [11]. It is noticeable that the best value of the A factor was achieved

Table 3. Selectivity data with respect to carbon balance during SHC-1 reaction in the presence of propane, hydrogen, oxygen and nitrogen

Catalysts	CO (%)	CO_2 (%)	CH_4 (%)	C_2H_4 (%)	C_2H_6 (%)	C_3H_8 (%)	Sum (%)
0.5Rh	26.4	30.7	5.0	18.1	9.6	10.2	100
0.5Rh-0.30Sn	26.0	29.8	5.2	19.2	9.8	10.0	100
0.5Rh-0.50Sn	25.1	29.1	5.2	19.3	11.3	10.0	100
0.5Rh-1.0Sn	24.7	28.8	5.3	19.6	10.7	10.9	100
0.5Rh-1.5Sn	18.7	19.4	5.3	16.9	7.2	32.5	100
0.5Rh-2.0Sn	20.0	20.3	6.3	21.9	12.2	19.3	100
0.5Rh-3.0Sn	20.7	20.8	6.2	22.5	13.3	16.5	100
1.5 Sn	47.2	51.6	0.2	0.5	0.4	0.1	100

Table 4. Conversions of hydrogen, oxygen, and propane presented with propylene selectivity and propylene yield (SHC-2)

Catalysts	H_2 conversion (%)	O_2 conversion (%)	C_3H_8 conversion (%)	Selectivity to propylene (%)	Yield of propylene (%)
0.5Rh-0.15Sn	66.0	94.9	24.2	85.5	20.6
0.5Rh-0.30Sn	65.7	95.0	24.6	85.6	21.1
0.5Rh-0.50Sn	66.6	94.9	25.2	85.8	21.6
0.5Rh-0.75Sn	66.2	94.9	25.5	85.9	21.9
0.5Rh-1.0Sn	76.7	94.8	26.5	87.2	23.1
0.5Rh-1.5Sn	78.0	94.8	28.9	89.5	25.9
0.5Rh-2.0Sn	79.0	95.0	28.1	87.9	24.7
0.5Rh-3.0Sn	79.2	96.0	28.0	87.4	24.4

Table 5. Selectivity data with respect to carbon balance after SHC-2 reaction in the presence of propane, hydrogen, oxygen and nitrogen

Catalysts	CO (%)	CO_2 (%)	CH_4 (%)	C_2H_4 (%)	C_2H_6 (%)	C_3H_6 (%)	Sum (%)
0.5Rh-0.15Sn	4.9	6.3	1.3	0.1	1.9	85.5	100
0.5Rh-0.30Sn	4.8	6.3	1.3	0.1	1.9	85.6	100
0.5Rh-0.50Sn	4.6	6.2	1.4	0.1	1.9	85.8	100
0.5Rh-0.75Sn	4.5	6.1	1.4	0.1	2.0	85.9	100
0.5Rh-1.0Sn	4.1	5.3	1.4	0.1	1.9	87.2	100
0.5Rh-1.5Sn	3.7	4.5	1.1	0.1	1.1	89.5	100
0.5Rh-2.0Sn	4.0	4.9	1.3	0.1	1.8	87.9	100
0.5Rh-3.0Sn	4.2	5.0	1.4	0.1	1.9	87.4	100

in 0.5Rh-1.5Sn catalyst. It should be noticed that the total hydrogen conversions contributed to hydrogen combustion and also hydrogenation.

2. Catalytic Performance for SHC-2 Reaction in Propane

Table 4 presents the conversion data of H_2, O_2, and propane for SHC-2 reaction. The range of H_2 conversion was from 65.7 to 79.2% in Rn-Sn catalysts, and the increase of H_2 conversion with increasing Sn amounts, which is similar pattern in SHC-1 reaction, was observed (Table 2). The sharp increase of H_2 conversion appeared from 0.5Rh-1.0Sn catalyst instead of 0.5Rh-1.5Sn in SHC-1 reaction after mild increases along with Sn additions to 0.5Rh catalyst. As also shown in SHC-1, there were no significant increases in H_2 conversion data for 0.5Rh-2.0Sn and 0.5Rh-3.0Sn. In terms of O_2 conversion, all Rh-Sn catalysts showed higher values from 94.8 to 96%. Regarding propane conversion, 0.5Rh-1.5Sn catalyst showed the highest value with highest propylene selectivity and propylene yield. If we also plot A factor for SHC-2 reaction, 0.5Rh-1.5Sn catalyst became the highest, as shown in SHC-1 reaction.

In Table 5 the generated products from SHC-2 reaction are recorded and presented. In fact, SHC-2 includes the effects of PDH and SHC together. PDH produces hydrogen as the process proceeds. In terms of hydrogen generation, additional hydrogen as a feed and hydrogen from PDH would compete in SHC-2 reaction. Compared with SHC-1 in Table 3, much less amount of CO and CO_2 was recorded as expected. Much larger amount of hydrogen in SHC-2 reaction compared with SHC-1, would be surely consumed by oxygen combustion, because there is no significant evidence of hydrogenation in SHC-2. Higher values in propylene provide the clue that SHC-2 option may be positively applicable to the current PDH reaction. Note that the hydrogen conversion data in Table 4 includes the generation of H_2O as well as the regain of

Table 6. Dispersion and surface area results obtained from CO chemisorption

Catalysts	Metal dispersion (%)	Metallic surface area (m^2/g metal)	Metallic surface area (m^2/g cat.)
0.5Rh	6.94	30.56	0.1528
0.5Rh-0.30Sn	10.15	45.27	0.2264
0.5Rh-0.50Sn	14.34	63.15	0.3158
0.5Rh-1.0Sn	33.70	110.33	0.5517
0.5Rh-1.5Sn	49.93	121.76	0.6088
0.5Rh-2.0Sn	19.67	86.60	0.4330
0.5Rh-3.0Sn	20.25	89.13	0.4456
1.5Sn	1.13	5.00	0.025

propane from propylene as suggested from SHC-1. Even though the conversion occurred from propylene to propane that is apparently unwanted reaction; however, the overall propylene production was increased in SHC-2 reaction.

3. Catalyst Characterization

3-1. CO Chemisorption

Table 6 shows the metal dispersion and surface area data through CO chemical adsorption. As Sn content increased to 1.5 wt% (0.5Rh-1.5Sn), the dispersion and surface area of metal also increased. However, the dispersion and the surface area of metal decreased as Sn amount increased more than 1.5 wt%. The 0.5Rh catalyst and the 1.5Sn catalyst had the lowest dispersion and specific surface area data. The result supports the highest A factor obtained with 0.5Rh-1.5Sn catalyst during SHC-1 reaction. Relative higher values in metal dispersion and metallic surface area in Table 6 provides the idea that both higher values are dependent upon the active metal amount, here, the content of Rh. The metal dispersion could be dependent on its loading amount. It was reported that the metal dispersion data of 3 wt% and 1 wt% of Pt loadings were about 4% and 12%, respectively, which supports the idea that the favorable dispersion occurred in lower metal loadings. Nevertheless, the values are much higher than the values in Pt loadings [25,26].

3-2. XPS Analysis

In Fig. 3, XPS spectra of 0.5Rh-1.5Sn and 0.5Rh-3.0Sn catalysts are presented in two states of fresh and used after SHC-1 reaction. The binding energies of the Sn 3d 5/2 peaks were 487 and 485 eV, and deconvolution was applied to compare the content of Sn(II, IV). Sn(II) and Sn(IV) represent the states of SnO and SnO_2, respectively. In case of fresh condition, the dominance of Sn(II) was noticeable for both 0.5Rh-1.5Sn and 0.5Rh-3.0Sn catalysts. After calcination for fresh catalysts, Sn oxides existed in two states of SnO and SnO_2. After SHC-1 reaction, the dominance of Sn(IV) was observed for both 0.5Rh-1.5Sn and 0.5Rh-3.0Sn catalysts. During SHC-1 reaction, oxygen can adsorb on the surface of metal and metal oxides. In this system, Rh and Sn oxides were major catalyst particles containing more active sites. Supposing that O_2 adsorbs only on the surface of Sn oxides apart from the surface of Rh, it would be possible that more O_2 adsorbed on the surface of SnO instead of SnO_2. Split O atom on the surface of SnO may contribute to convert H_2 to H_2O. Subsequently, it could be possible that remaining O atom after combustion contributes to form SnO_2 from SnO. Meanwhile, the conversions to both CO and CO_2 could be occurring mainly on the surface of Rh particles rather than the surface of SnO.

3-3. TEM-EDS Mapping Images

TEM-EDS mapping images of 0.5Rh-1.5Sn and 0.5Rh-3.0Sn catalysts are presented before and after SHC-1 reaction in Fig. 4. It can be seen that the Rh particles were aggregated after SHC-1 reaction in both 0.5Rh-1.5Sn and 0.5Rh-3.0Sn catalysts. In both cases of 0.5Rh-1.5Sn and 0.5Rh-3.0Sn catalysts, the aggregation of Rh particles was observed. The size of green distributed dots became larger after SHC-1 reaction, which shows the sintering of Rh particles. Meanwhile, the sizes of Sn oxides in 0.5Rh-1.5Sn, red distributed dots, did not grow much after SHC-1 compared with 0.5Rh-3.0Sn catalyst. More dispersion and higher values in 0.5Rh-1.5Sn catalyst is consistent with CO chemisorption data in Table 6.

3-4. Temperature Program Reduction Analysis (TPR)

Fig. 5 shows TPR profiles of Rh-Sn catalysts and monometallic

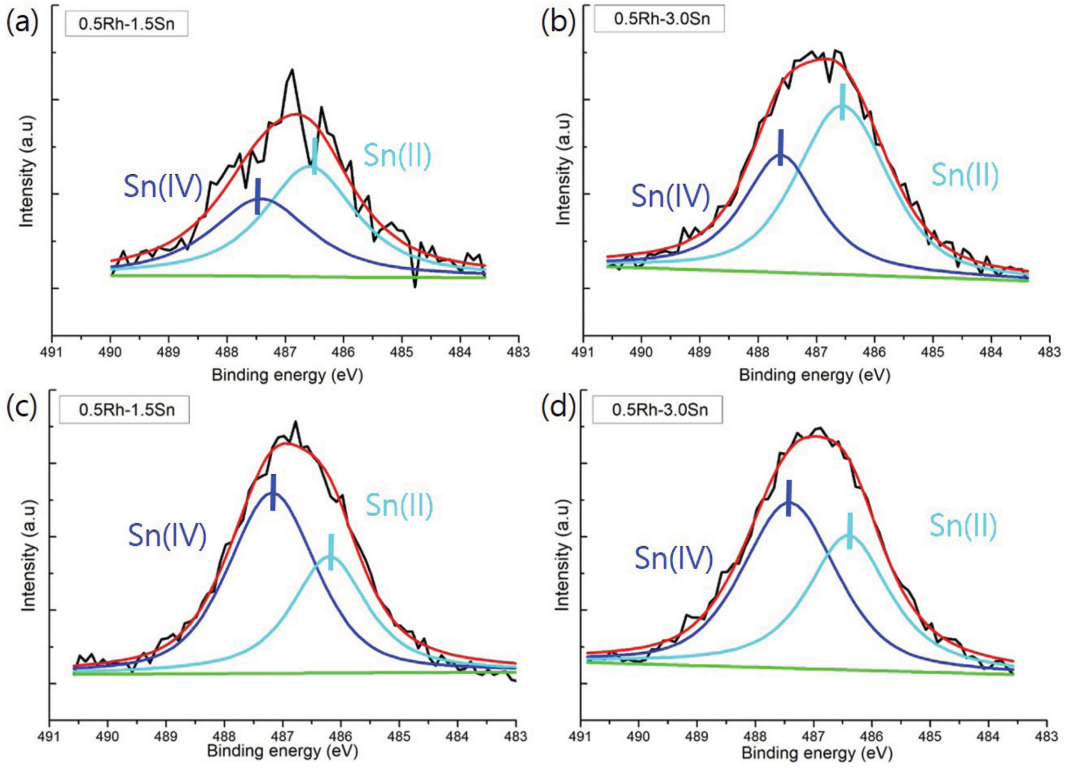

Fig. 3. XPS spectra of fresh 0.5Rh-1.5Sn (a) and fresh 0.5Rh-3.0Sn (b), and 0.5Rh-1.5Sn after SHC-1 (c) and 0.5Rh-3.0Sn after SHC-1 (d).

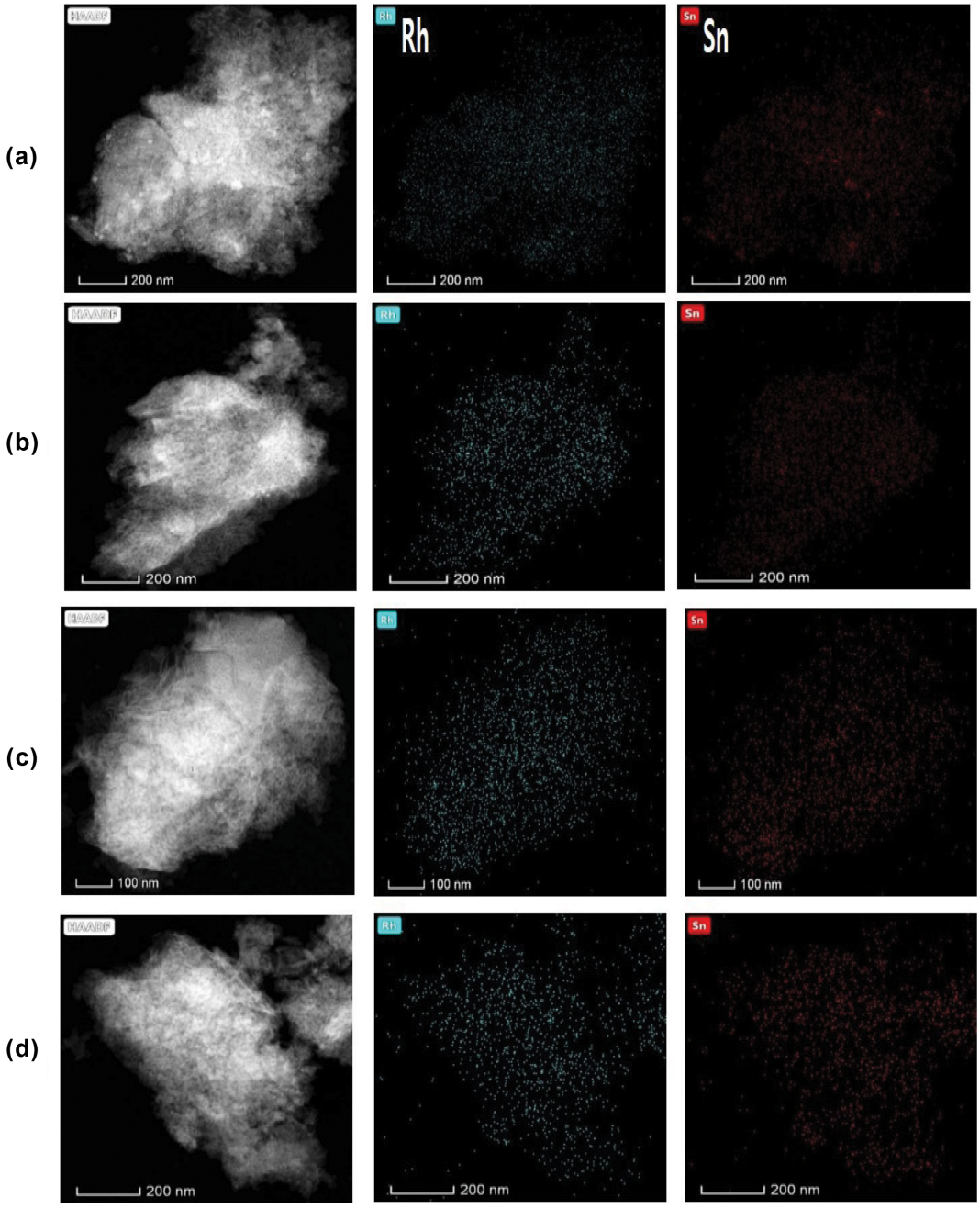

Fig. 4. TEM-EDX mapping images of 0.5Rh-1.5Sn and 0.5Rh-3.0Sn catalysts: (a) Fresh 0.5Rh-1.5Sn, (b) 0.5Rh-1.5Sn after SHC-1 reaction, (c) 0.5Rh-3.0Sn, and (d) 0.5Rh-3.0Sn after SHC-1 reaction.

0.5Rh and 1.5Sn catalysts. TPR profile of 0.5Rh shows two noticeable peaks at around 200 °C and 470 °C. Sheerin et al. [27] examined that the appearance of two major TPR peaks from Rh/CeO_2 catalyst was by the reduction of Rh states as well as support. They reported that TPR peaks were attributed to the reduction from Rh^{3+} to Rh^{1+} at 25 °C and combined effect of Rh^{1+} to Rh^0 and CeO_2 reduction at 75 °C, respectively. Low TPR value of CeO_2 reduction that is often reported up to 500 °C for surface reduction was interpreted by the effect of interactions between Rh and CeO_2 [27]. Returning to Fig. 5, the peak at 200 °C may be attributed to the effect of Rh reduction, such as the reduction from Rh^+ to Rh^0, and the peak at 470 °C may be accounted to the reduction effect between metal and alumina surface [28,29]. With increasing the amounts of Sn into 0.5Rh catalyst, two TPR peaks more or less appeared at temperatures between 200 °C and 470 °C. The distance between two peaks was even closer when Sn amount reached 1.5 wt%. In case of 0.5Rh-3.0Sn catalyst, it became harder to distinguish two TPR peaks. Compared to a broad TPR curve for 1.5Sn catalyst, the effect of Sn for 0.5Rh-3.0Sn catalyst looks more dominant and that may shadow the effect of Rh. This suggests that the role of Rh states is important to maintain catalyst activity for both SHC reactions. Higher content of Sn may partially cover the effect

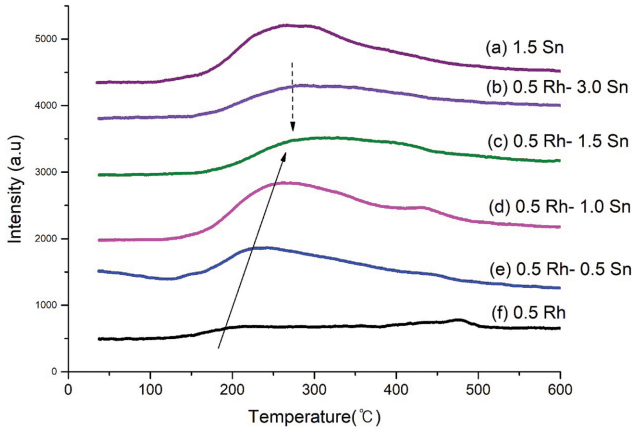

Fig. 5. TPR profile of catalysts.

of active Rh sites and decrease catalytic performance.

CONCLUSION

A series of Rh-Sn catalysts were prepared by fixed amount of Rh and varied amounts of Sn. Two selective hydrogen combustion reactions, SHC-1 and SHC-2, were evaluated in the presence of propylene, hydrogen, oxygen, and nitrogen for SHC-1 and propane, hydrogen, oxygen, and nitrogen for SHC-2, respectively. During SHC-1 reaction, carbons in propylene converted to CO, CO_2, methane, ethane, ethylene, and propane. The combined amount of CO and CO_2 was suddenly decreased when 0.5Rh-1.5Sn catalyst was used in SHC-1. In addition, 0.5Rh-1.5Sn showed an increase of propylene conversion, which should be carefully analyzed. It was interpreted that the total consumption of propylene contributes in two ways: combustion and hydrogenation. Here, hydrogenation also plays an important role of the generation of methane, ethane, ethylene, and propane. If propane is generated during SHC-1, hydrogen conversion may also attribute the return of propane from propylene. Nevertheless, SHC-1 reduces the total combustion of carbons. The highest value in propane generation in 0.5Rh-1.5Sn was proposed by metal dispersion, which was supported by CO chemisorption section. The term, A factor, was introduced by the ratio of H_2 conversion to propylene conversion. It is noticeable that the best value of A factor was achieved in 0.5Rh-1.5Sn catalyst. In case of SHC-2 reaction, the range of H_2 conversion was from 65.7 to 79.2% in Rn-Sn catalysts, and observed the increases of H_2 conversion with increasing Sn amount, which is a similar pattern in the SHC-1 reaction. Regarding propane conversion, 0.5Rh-1.5Sn catalyst also showed the highest value with highest propylene selectivity and propylene yield. If we also count the A factor for SHC-2 reaction, 0.5Rh-1.5Sn catalyst also became the highest, as shown in SHC-1 reaction. In fact, SHC-2 includes the effects of PDH and SHC together. PDH produces hydrogen as it occurs. Additional hydrogen as a feed and also hydrogen from PDH would compete in SHC-2 reactions. Compared with SHC-1, much less amounts of CO and CO_2 were recorded in SHC-2. Much larger amount of hydrogen in SHC-2 reaction compared with SHC-1, would be consumed mainly by oxygen combustion. This is because there is no significant evidence of hydrogenation in SHC-2. Even though the conversion occurred from propylene to propane, that is an unwanted reaction in terms of SHC; however, the overall propylene production that we wanted was increased in the SHC-2 reaction.

ACKNOWLEDGEMENTS

This work was financed by an industry core-technology project called "Development of high yield propylene production process technology" of the Ministry of Trade, Industry and Energy (project No.: 100052754-Korea Evaluation Institute of Industrial Technology). This work was also financed by Basic Science Research Program through the National Research Foundation of Korea (NRF) funded by the Ministry of Education (2017R1D1A1B03034244).

REFERENCES

1. H. H. Kung, in edited by D. D. Eley, H. Pines and W. O. B. T.-A. in C. Haag. *Adv. Catal.*, **40**, 1 (1994).
2. M. M. Bhasin, J. H. McCain, B. V Vora, T. Imai and P. R. Pujadó, *Appl. Catal. A Gen.*, **221**, 397 (2001).
3. L. M. Madeira and M. F. Portela, *Catal. Rev.*, **44**, 247 (2002).
4. S. Bocanegra, A. Ballarini, P. Zgolicz, O. Scelza and S. de Miguel, *Catal. Today*, **143**, 334 (2009).
5. S. Sahebdelfar, M. T. Ravanchi, F. Tahriri Zangeneh, S. Mehrazma and S. Rajabi, *Chem. Eng. Res. Des.*, **90**, 1090 (2012).
6. B. V. Vora, *Top. Catal.*, **55**, 1297 (2012).
7. C.-H. Lin, K.-C. Lee and B.-Z. Wan, *Appl. Catal. A Gen.*, **164**, 59 (1997).
8. L. Låte, J.-I. Rundereim and E. A. Blekkan, *Appl. Catal. A Gen.*, **262**, 53 (2004).
9. O. Czuprat, J. Caro, V. A. Kondratenko and E. V. Kondratenko, *Catal. Commun.*, **11**, 1211 (2010).
10. D. Creaser, B. Andersson, R. R. Hudgins and P. L. Silveston, *Appl. Catal. A Gen.*, **187**, 147 (1999).
11. R. Liu, Y. Zhu, Z. Sui, H. Wang, P. Li and X. Zhou, *Fuel Process. Technol.*, **108**, 82 (2013).
12. L. Låte, W. Thelin and E. A. Blekkan, *Appl. Catal. A Gen.*, **262**, 63 (2004).
13. R. K. Grasselli, D. L. Stern and J. G. Tsikoyiannis, *Appl. Catal. A Gen.*, **189**, 1 (1999).
14. E. V. Shelepova, A. A. Vedyagin, I. V. Mishakov and A. S. Noskov, *Chem. Eng. J.*, **176-177**, 151 (2011).
15. H. Lee, W. I. Kim, K. D. Jung and H. L. Koh, *Korean J. Chem. Eng.*, **34**, 1337 (2017).
16. R. Hu, X. Li, Z. Sui, G. Ye and X. Zhou, *Chem. Eng. Process. - Process Intensif.*, **143**, 107608 (2019).
17. R. K. Grasselli, D. L. Stern and J. G. Tsikoyiannis, *Appl. Catal. A Gen.*, **189**, 1 (1999).
18. J. G. Tsikoyiannis, D. L. Stern and R. K. Grasselli, *J. Catal.*, **184**, 77 (1999).
19. H. Dyrbeck, N. Hammer, M. Rønning and E. A. Blekkan, *Top. Catal.*, **45**, 21 (2007).
20. M. J. O'Hara, T. Imai, J. C. Bricker and D. E. Mackowiak, US Patent, 4,565,898 (1986).
21. S. Kaneko, T. Arakawa, M. aki Ohshima, H. Kurokawa and H.

Miura, *Appl. Catal. A Gen.*, **356**, 80 (2009).
22. J. H. Blank, J. Beckers, P. F. Collignon, F. Clerc and G. Rothenberg, *Chem. - A Eur. J.*, **13**, 5121 (2007).
23. S. Liu, S. Gong, H. Feng, Z. Ma, L. Yang and P. Li, *Int. J. Hydrogen Energy*, **45**, 12347 (2020).
24. M. M. Montemore, M. A. van Spronsen, R. J. Madix and C. M. Friend, *Chem. Rev.*, **118**, 2816 (2018).
25. G. H. Kim, K. D. Jung, W. I. Kim, B. H. Um, C. H. Shin, K. Oh and H. L. Koh, *Res. Chem. Intermed.*, **42**, 351 (2016).
26. Y. S. Choi, K. Oh, K. D. Jung, W. I. Kim and H. L. Koh, *Catalysts*, **10**, 898 (2020).
27. O. A. Bariås, A. Holmen and E. A. Blekkan, *J. Catal.*, **158**, 1 (1996).
28. M. J. Kim, Y. J. Kim, S. J. Lee, I. S. Ryu, H. J. Kim, Y. Kim, C. H. Ko and S. G. Jeon, *Chem. Eng. Re. Des.*, **141**, 455 (2019).
29. N. D. Charisiou, C. Italiano, L. Pino, V. Sebastian, A. Vita and M. A. Goula, *Renew. Energy*, **162**, 908 (2020).